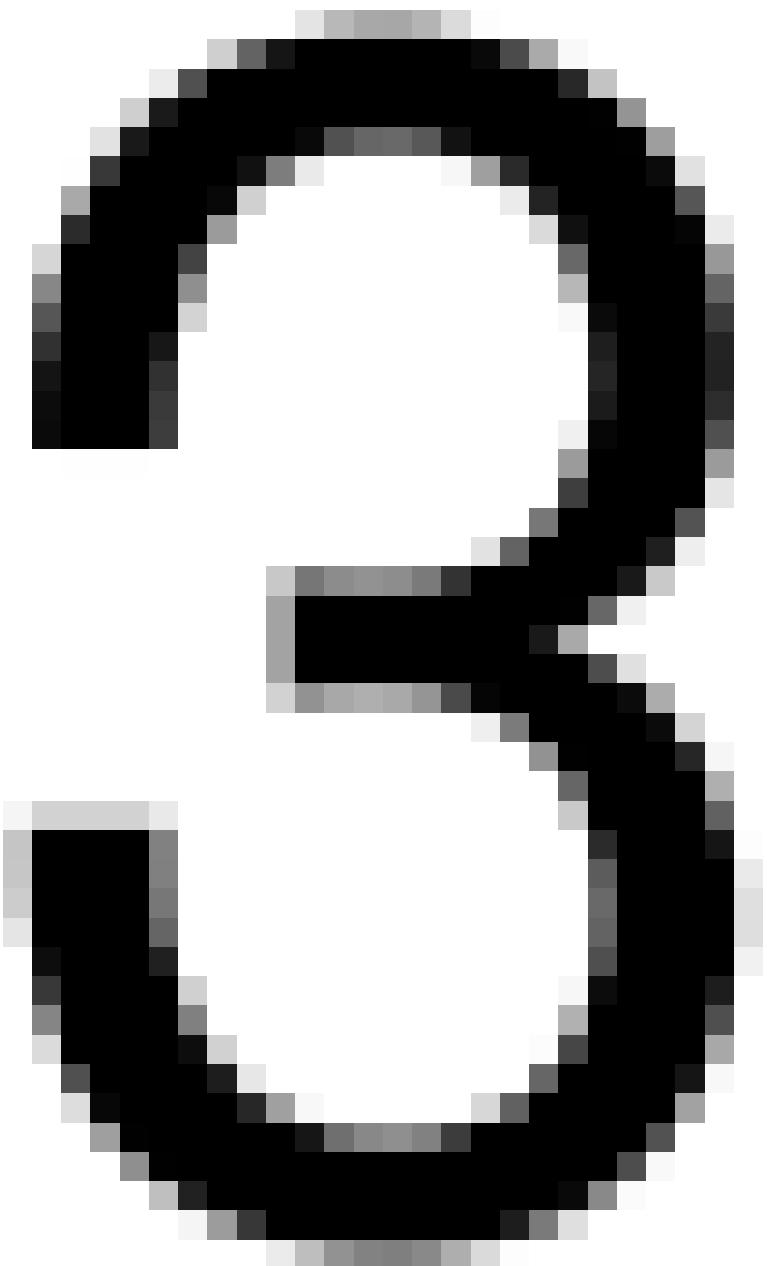


Montreal, Quebec, Canada, November 3rd, 2025 - A conference was held in Montreal, Quebec, Canada, on November 3rd, 2025. The conference was organized by the Canadian Association of Neuroscience and Psychology (CANP) and the Canadian Society for Neuroscience (CSN). The purpose of the conference was to bring together researchers, scientists, and professionals from various fields of neuroscience and psychology to share their latest findings and discuss future research directions. The conference featured several keynote speeches, panel discussions, and poster presentations. The attendees included students, postdoctoral fellows, and faculty members from universities and research institutions across Canada and abroad. The conference was a success and provided a valuable opportunity for networking and collaboration among the scientific community.



rectinnotopy

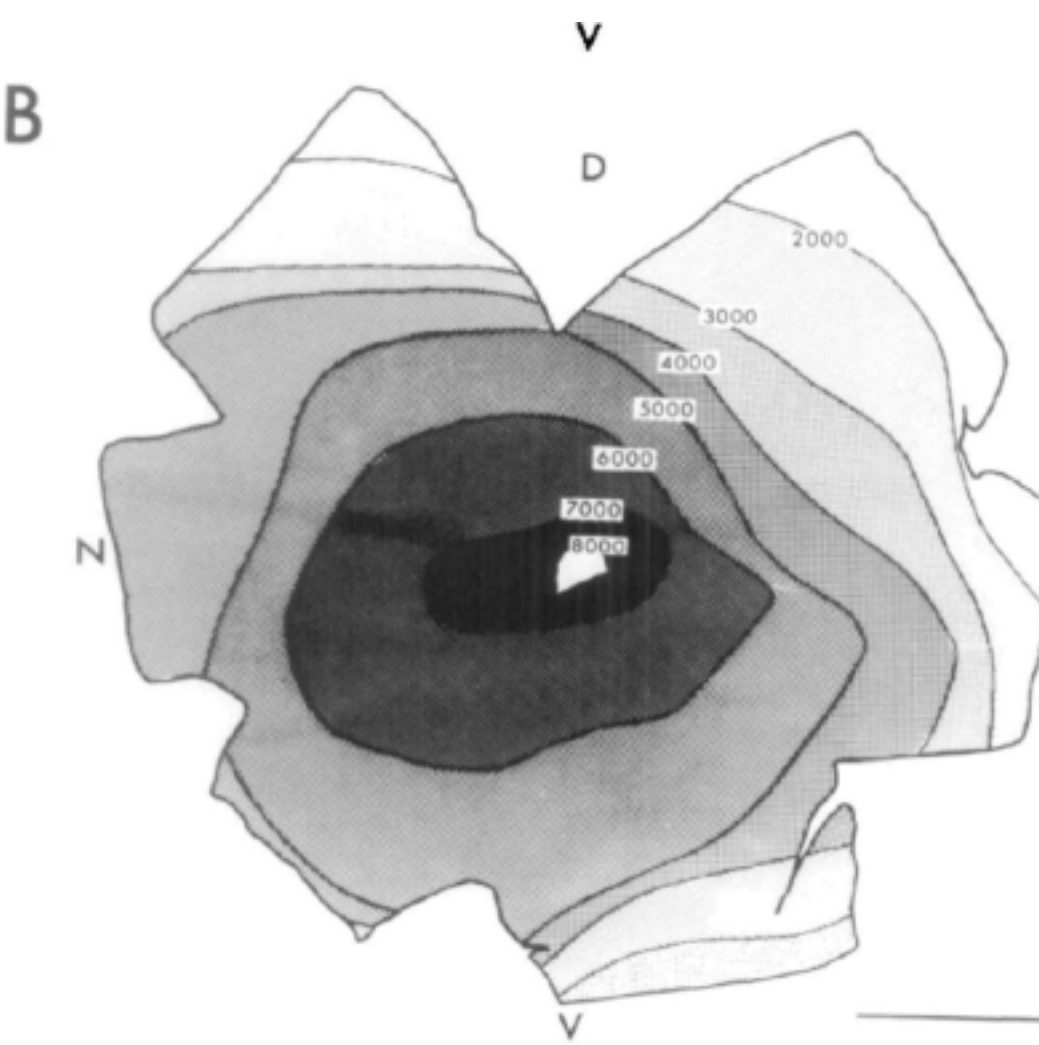
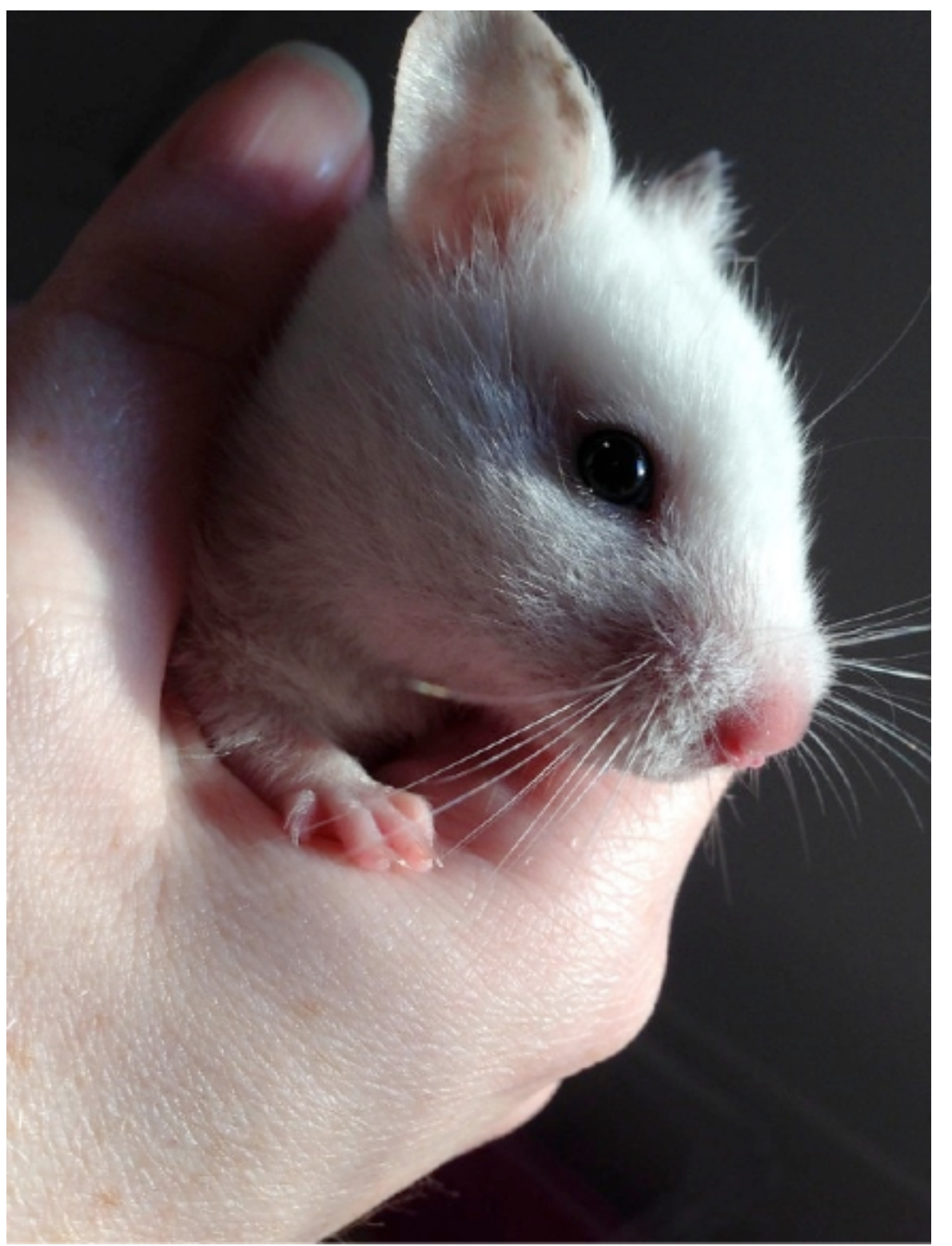
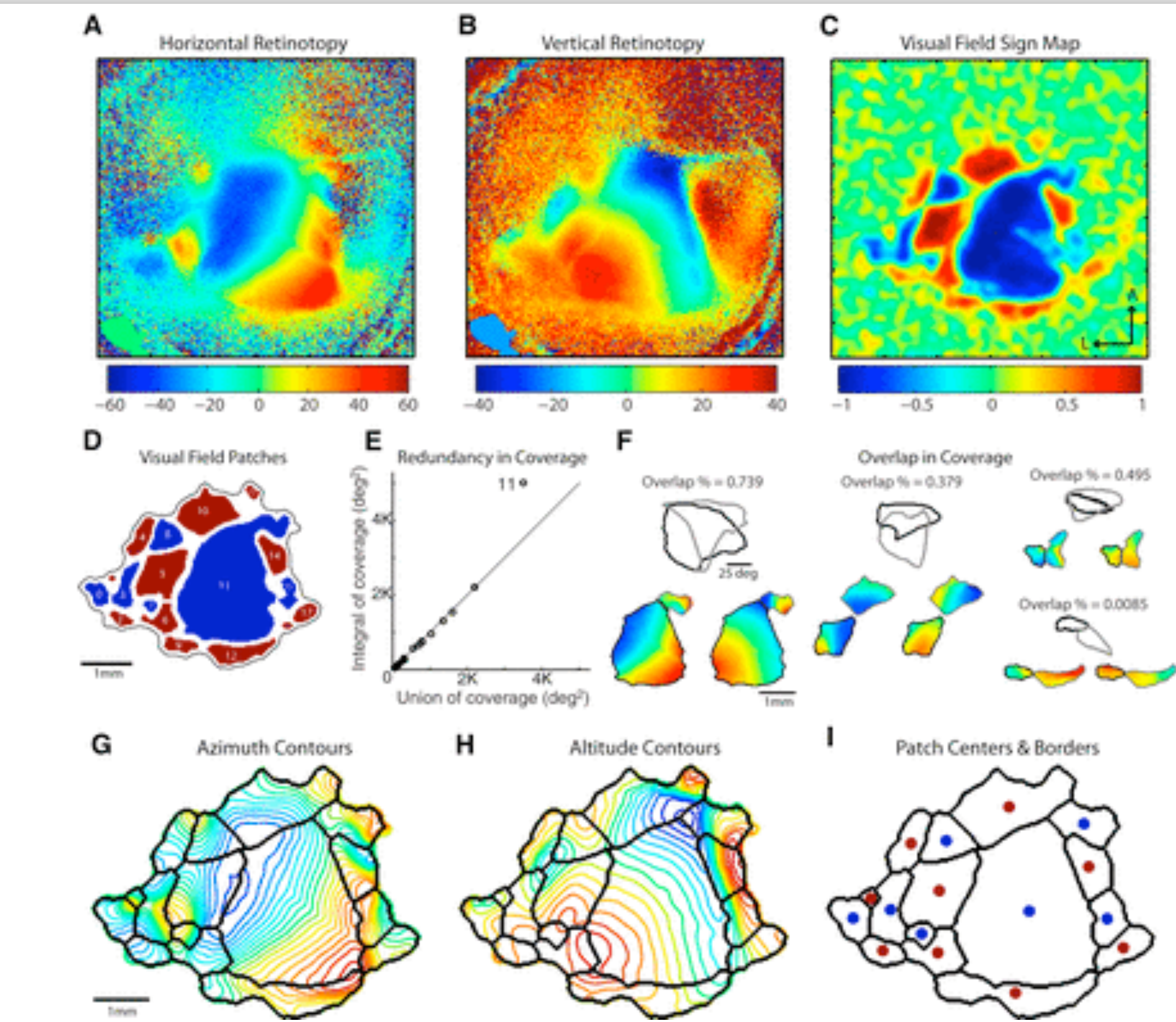


Fig. 3. Outline of retina. **A**, Density of presumed ganglion cells in cells per square millimeter for 76 locations. **B**, Summary of isodensity pattern. *D*, dorsal; *V*, ventral; *N*, nasal; *T*, temporal. (Bar = 1 mm.)

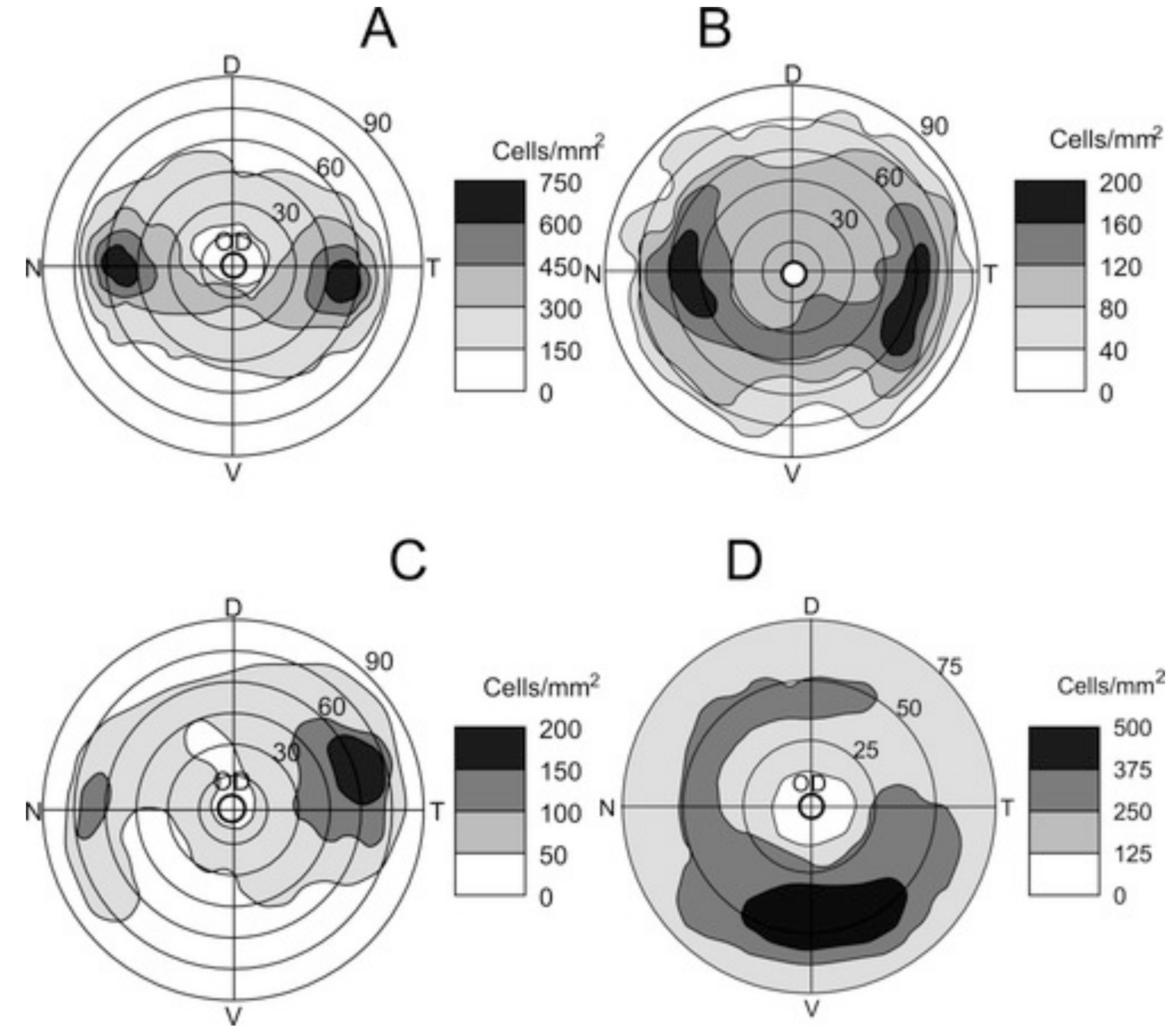


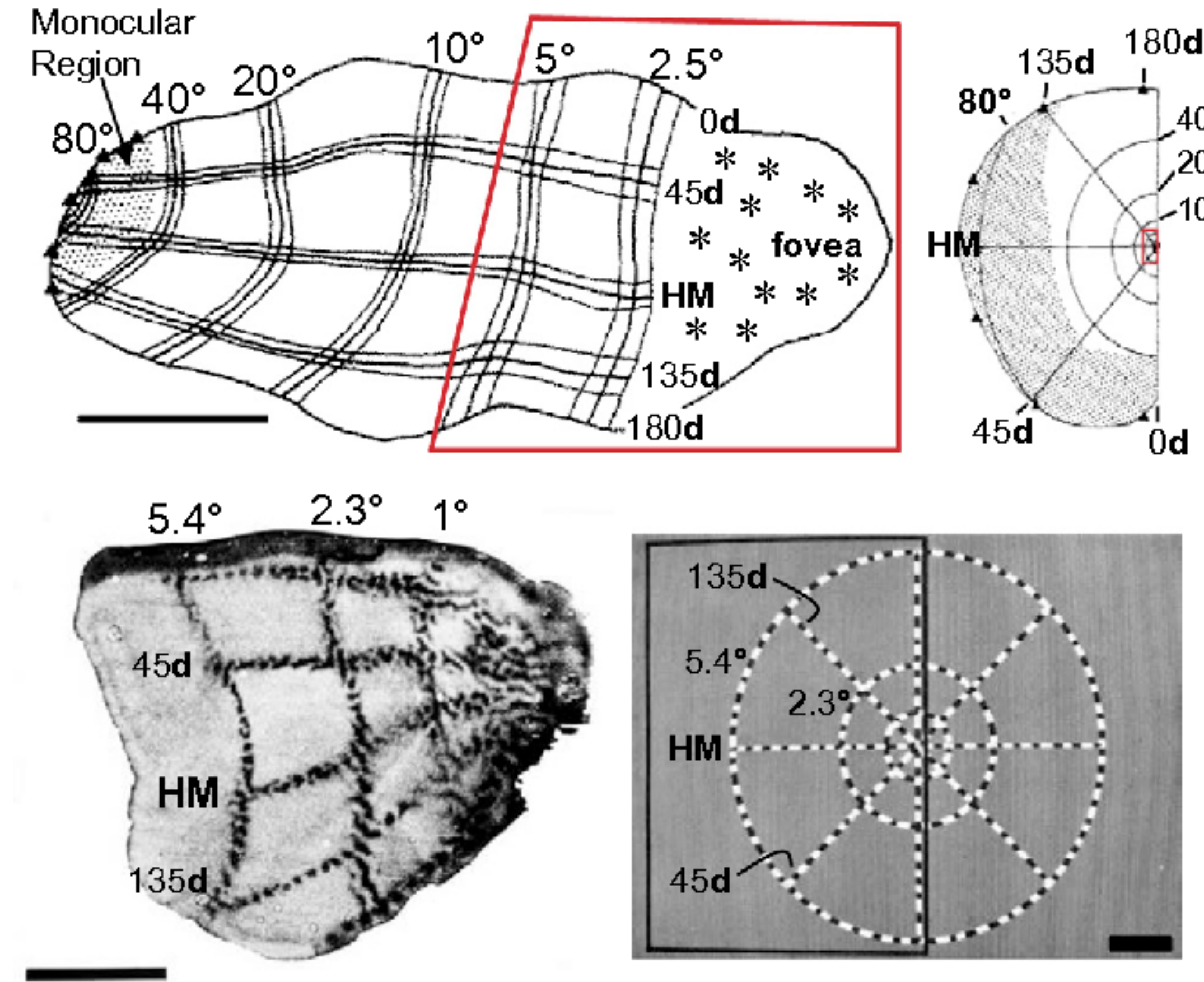
Topography and Areal Organization of Mouse Visual Cortex

Marina E. Garrett, Ian Nauhaus, James H. Marshel and Edward M. Callaway



A–D: Topographic distribution of ganglion cell density in the retina of some cetaceans: the bottlenose dolphin (A), the riverine tucuxi (B), the grey whale (C), and the Amazon river dolphin (D). Cell density is expressed as number of cells per mm^2 and is shown by various shadowing, according to the scales. Concentric circles show angular coordinates on a retinal hemisphere centered on the lens. D, V, N, T, dorsal, ventral, nasal, and temporal poles of the retina, respectively. in *Adaptive features of aquatic mammals' eye* Alla M. Mass, Alexander YA. Supin (2007) <https://doi.org/10.1002/ar.20529>





Retinotopic organization of macaque primary visual cortex. Top: Topography of V1 mapped with microelectrode recordings, from Van Essen, Newsome, and Maunsell (1984). Bottom: Topography of peri-foveal V1 mapped using 2-deoxyglucose functional labeling, from Tootell et al. (1988). Scale bars: top left, 1 cm; bottom left, 1 cm; bottom right, 2 cm.

From *Cortical magnification plus cortical plasticity equals vision?* (2015) R. Born, Alexander R. Trott and Till S.

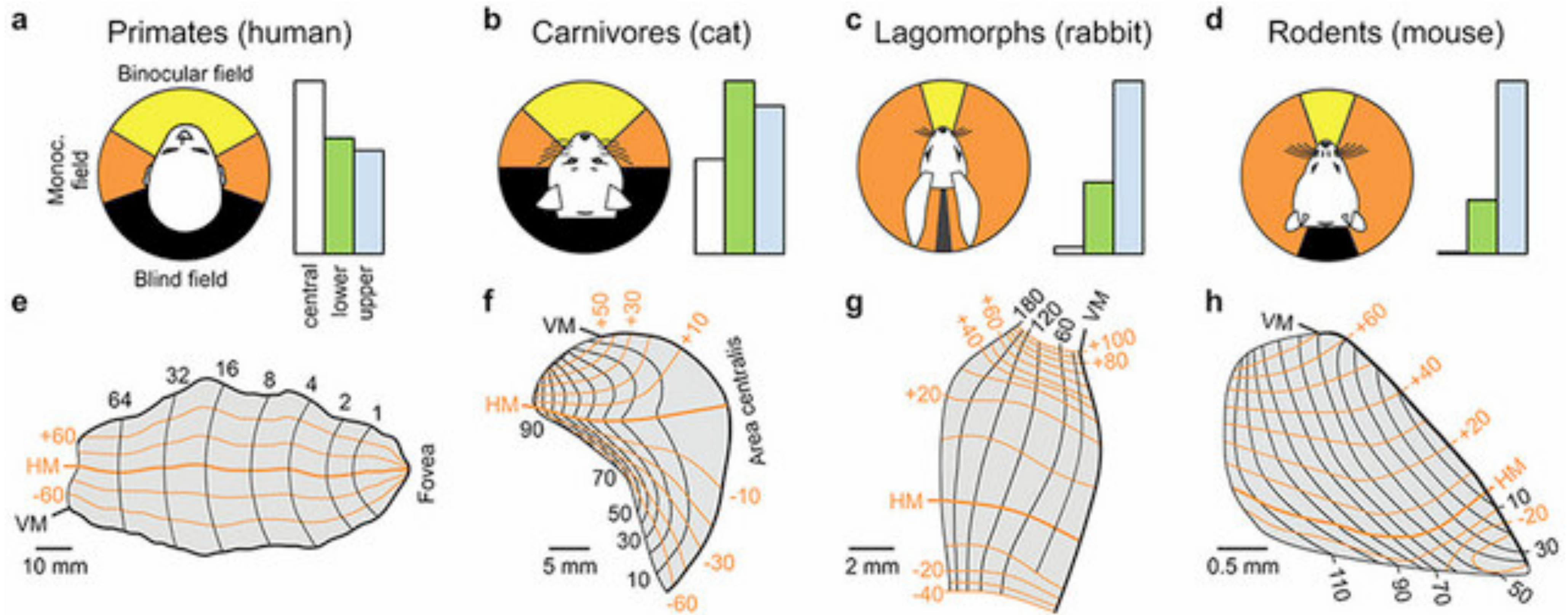


Figure 6. Cortical map for retinotopy. a-d. Visual fields and their cortical representation in humans (a), cats (b), rabbits (c) and mice (d). The left panel shows the binocular field (yellow), monocular field (orange) and the blind field (black). Values from (Mazade & Alonso 2017). The right panel shows the percentage of area V1 devoted to central vision (white, central 10 degrees), lower (green) and upper visual fields (blue). Percentages of blue bars are 26% (a), 36% (b), 69% (c), and 76% (d). Values obtained from retinotopic maps in e-h. e-h. Retinotopic maps of area V1 in the human, cat, rabbit and mouse. Redrawn from (Adams et al 2007) for a, (Tusa et al 1978) for b, (Hughes 1971) for c, and (Ji et al 2015) for d.

in: *Thalamocortical Circuits and Functional Architecture* (2018) Jens Kremkow, Jose-Manuel Alonso



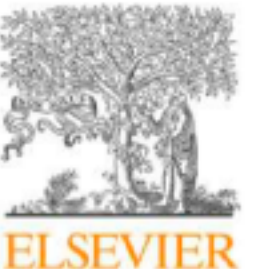
Article

End-to-end topographic networks as models of cortical map formation and human visual behaviour

Received: 21 August 2023

Zejin Lu^{1,2,7}✉, Adrien Doerig^{3,7}, Victoria Bosch^{1,7}, Bas Krahmer⁴, Daniel Kaiser^{5,6,8}, Radoslaw M. Cichy^{2,8} & Tim C. Kietzmann^{1,8}✉

Accepted: 17 April 2025



Robotics and Autonomous Systems 58 (2010) 378–398
 Contents lists available at ScienceDirect
Robotics and Autonomous Systems
 journal homepage: www.elsevier.com/locate/robot

A review of log-polar imaging for visual perception in robotics

V. Javier Traver^{a,b,*}, Alexandre Bernardino^c

a Orientation selectivity in layer 1

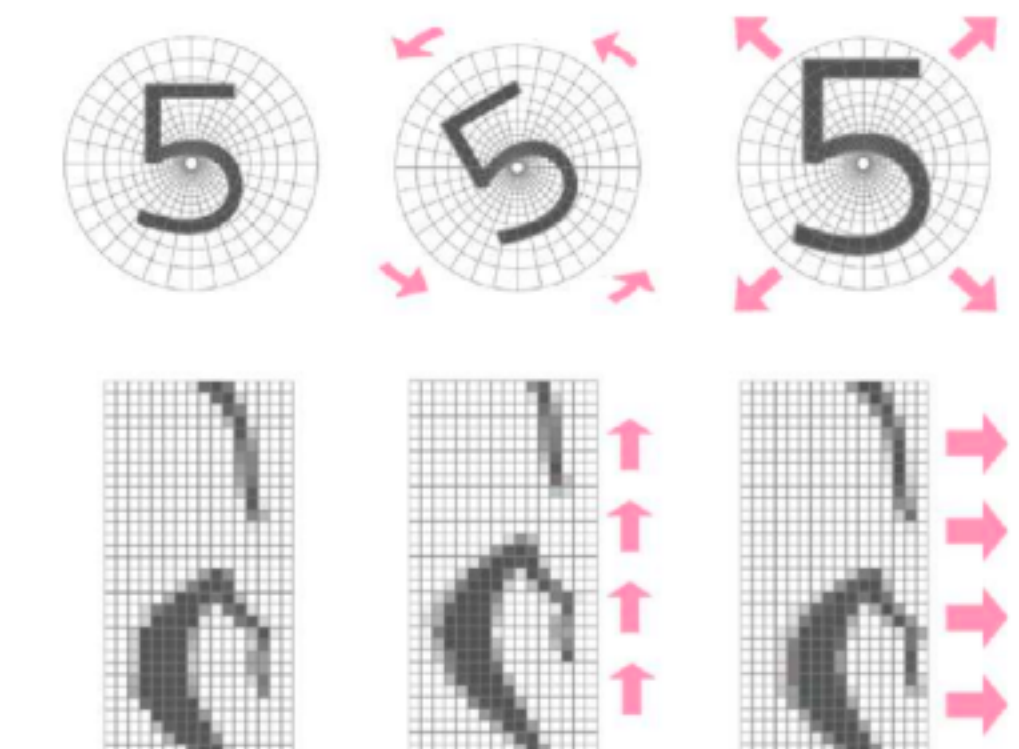
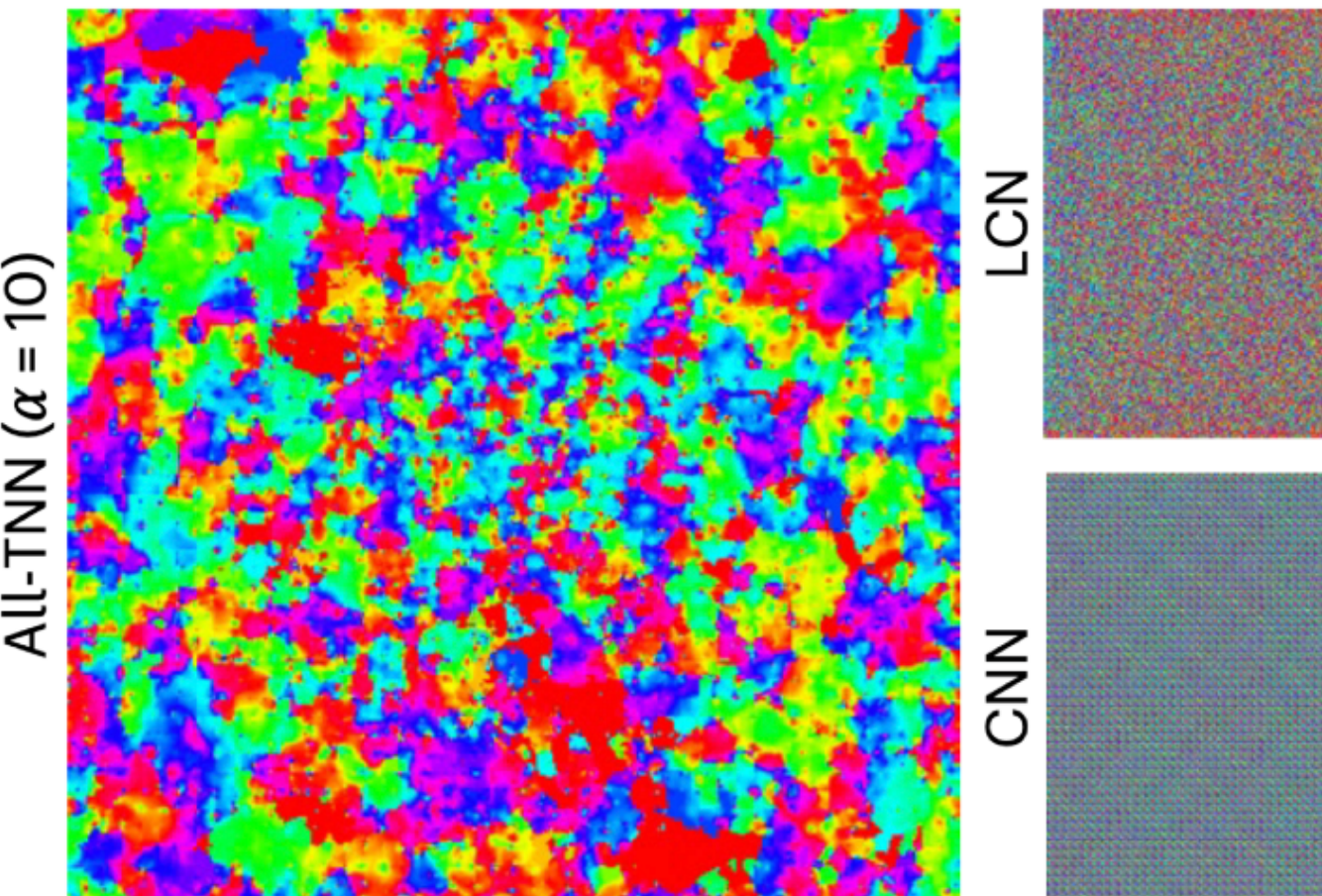


Fig. 3. Top: Retinal images on the log-polar mapping template. Bottom: The corresponding log-polar images. To illustrate the edge invariance property, the image on the left is rotated (middle) and scaled (right), which correspond to approximate translations in the log-polar domain, in the angular (η) and radial (ξ) directions, respectively, as shown with the arrows.

a

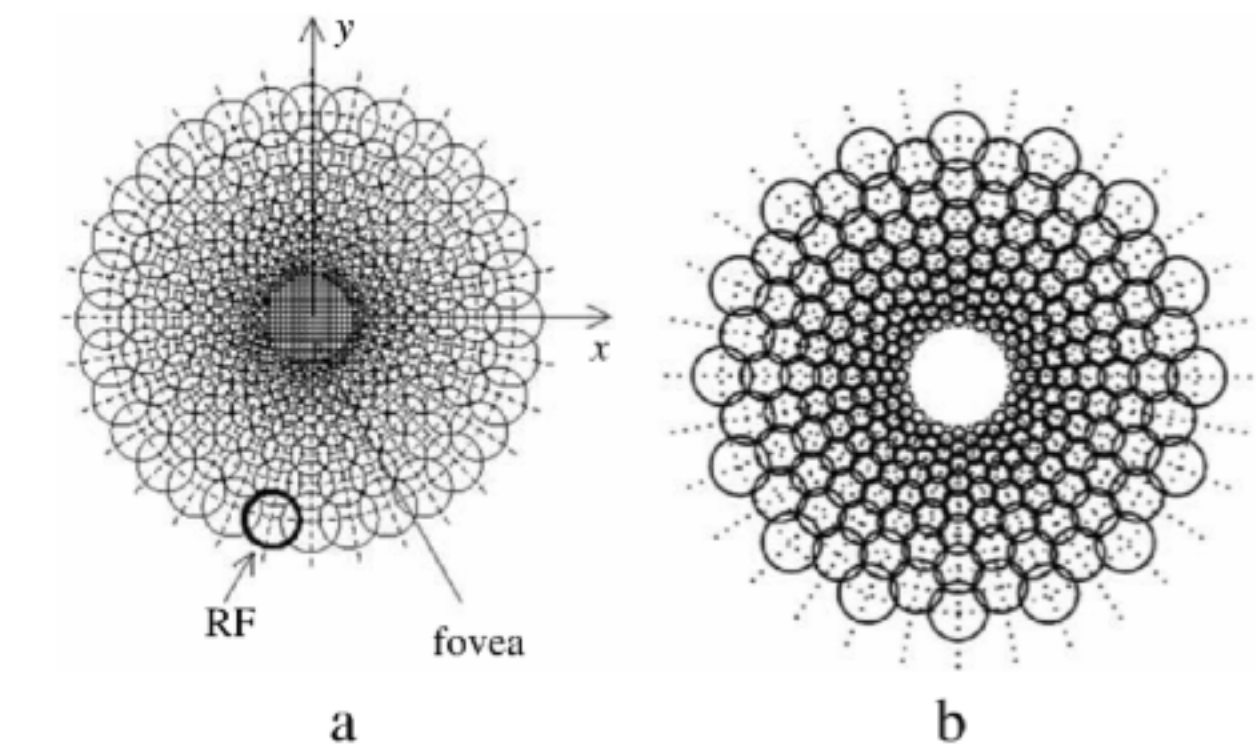


Fig. 4. Overlapping models: (a) the model of [29] implemented in [31], and (b) the model in [30] (figure taken from [16]).²

Retinotopy

nature human behaviour

Article

<https://doi.org/10.1038/s41562-025-02220-7>

End-to-end topographic networks as models of cortical map formation and human visual behaviour

Received: 21 August 2023

Zejin Lu  , Adrien Doerig  , Victoria Bosch  , Bas Krahmer⁴,

Accepted: 17 April 2025

Daniel Kaiser  , Radoslaw M. Cichy  & Tim C. Kietzmann  



Robotics and Autonomous Systems 58 (2010) 378–398

Contents lists available at ScienceDirect

Robotics and Autonomous Systems

journal homepage: www.elsevier.com/locate/robot

A review of log-polar imaging for visual perception in robotics

V. Javier Traver^{a,b,*}, Alexandre Bernardino^c

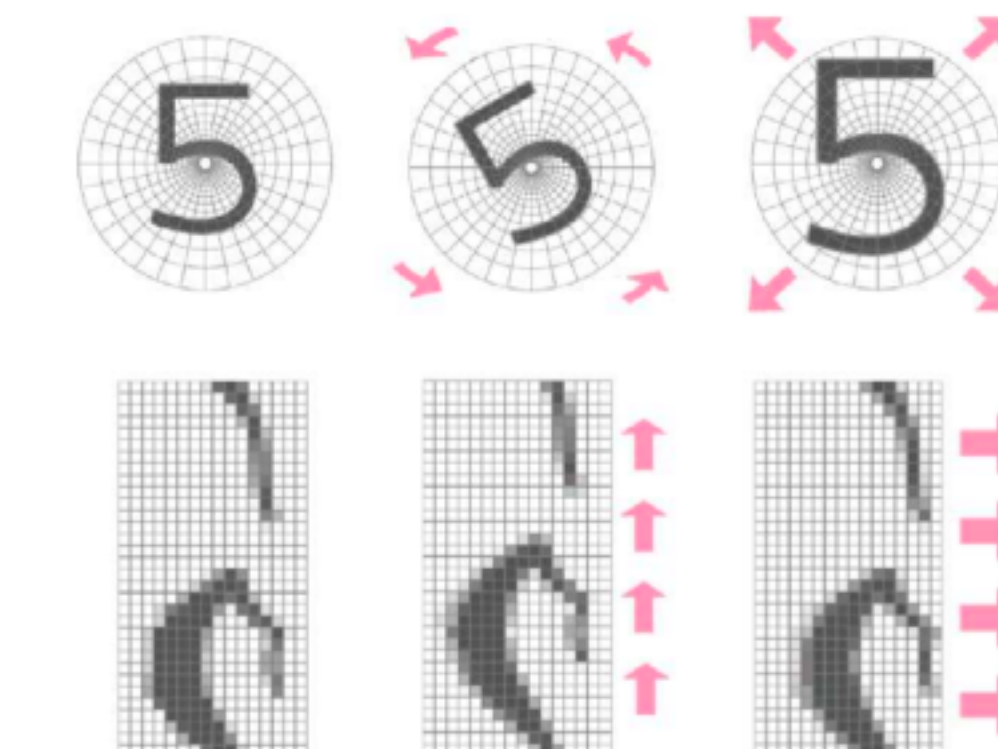


Fig. 3. Top: Retinal images on the log-polar mapping template. Bottom: The corresponding log-polar images. To illustrate the edge invariance property, the image on the left is rotated (middle) and scaled (right), which correspond to approximate translations in the log-polar domain, in the angular (η) and radial (ξ) directions, respectively, as shown with the arrows.

a Orientation selectivity in layer 1

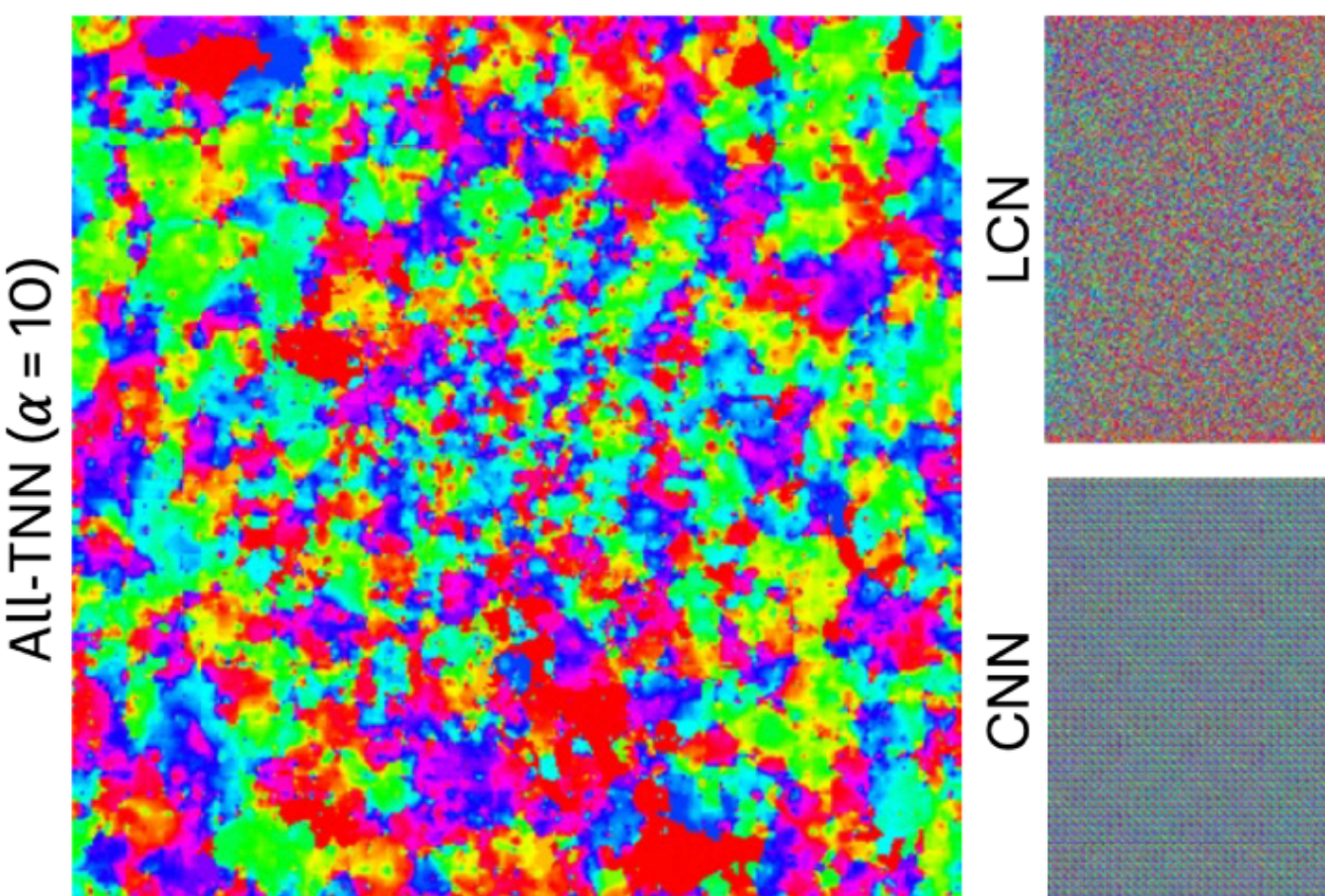


Fig. 4. Overlapping models: (a) the model of [29] implemented in [31], and (b) the model in [30] (figure taken from [16]).²

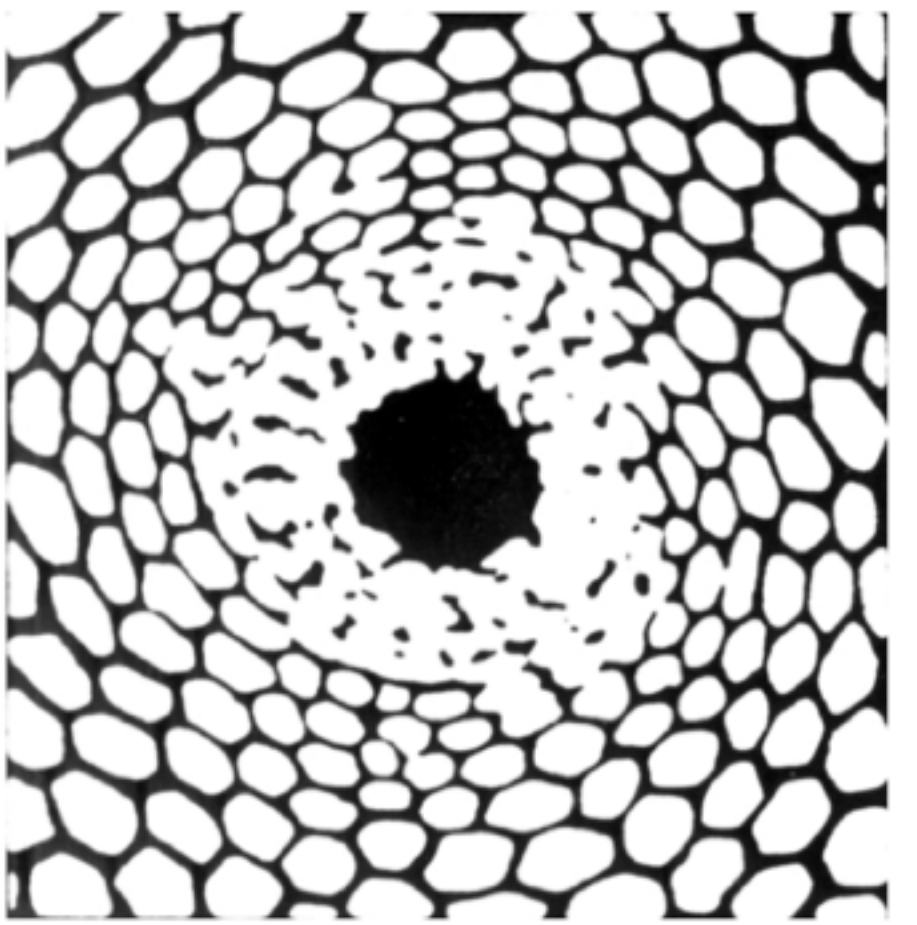


Figure 1. (a) ‘Phosphene’ produced by deep binocular pressure on the eyeballs. Redrawn from Tyler (1978).
(b) Honeycomb hallucination generated by marijuana. Redrawn from Clottes & Lewis-Williams (1998).

THE ROYAL
SOCIETY

Geometric visual hallucinations, Euclidean symmetry and the functional architecture of striate cortex

Paul C. Bressloff¹, Jack D. Cowan^{2*}, Martin Golubitsky³,
Peter J. Thomas⁴ and Matthew C. Wiener⁵

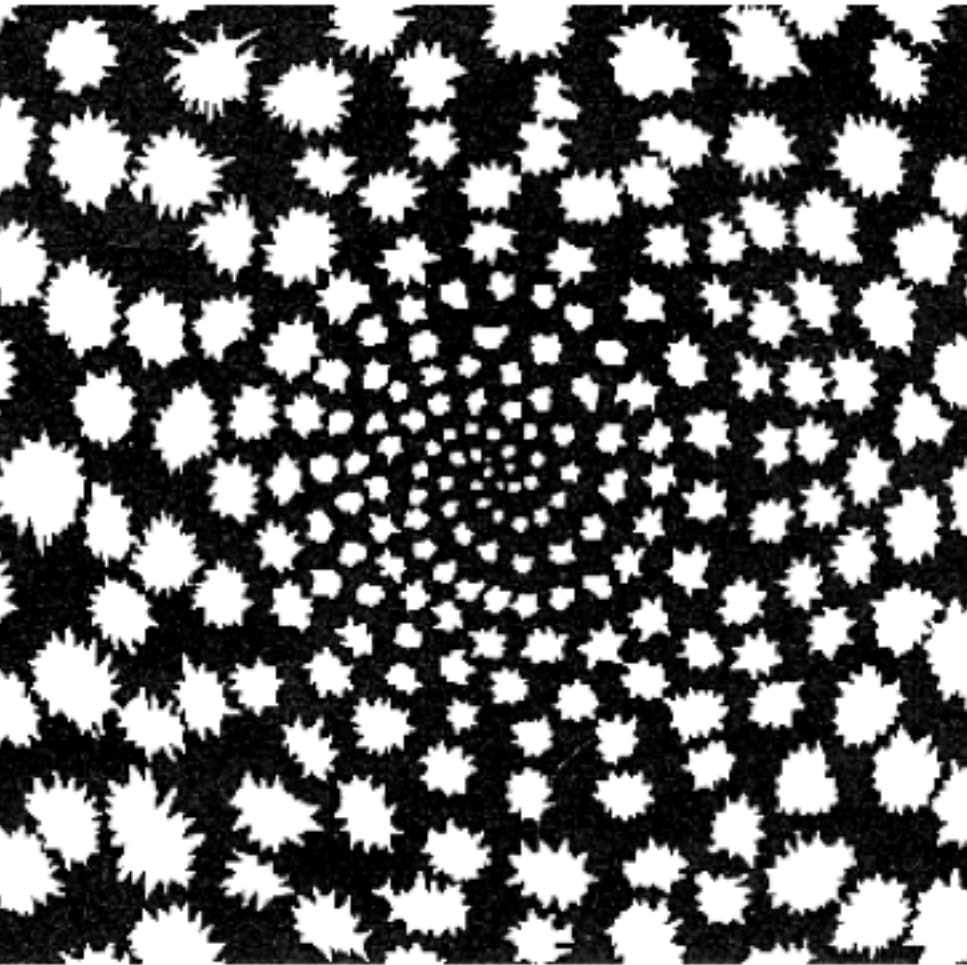


Figure 3. (a) Funnel and (b) spiral tunnel hallucinations generated by LSD. Redrawn from Siegel (1977).

doi 10.1098/rstb.2000.0769

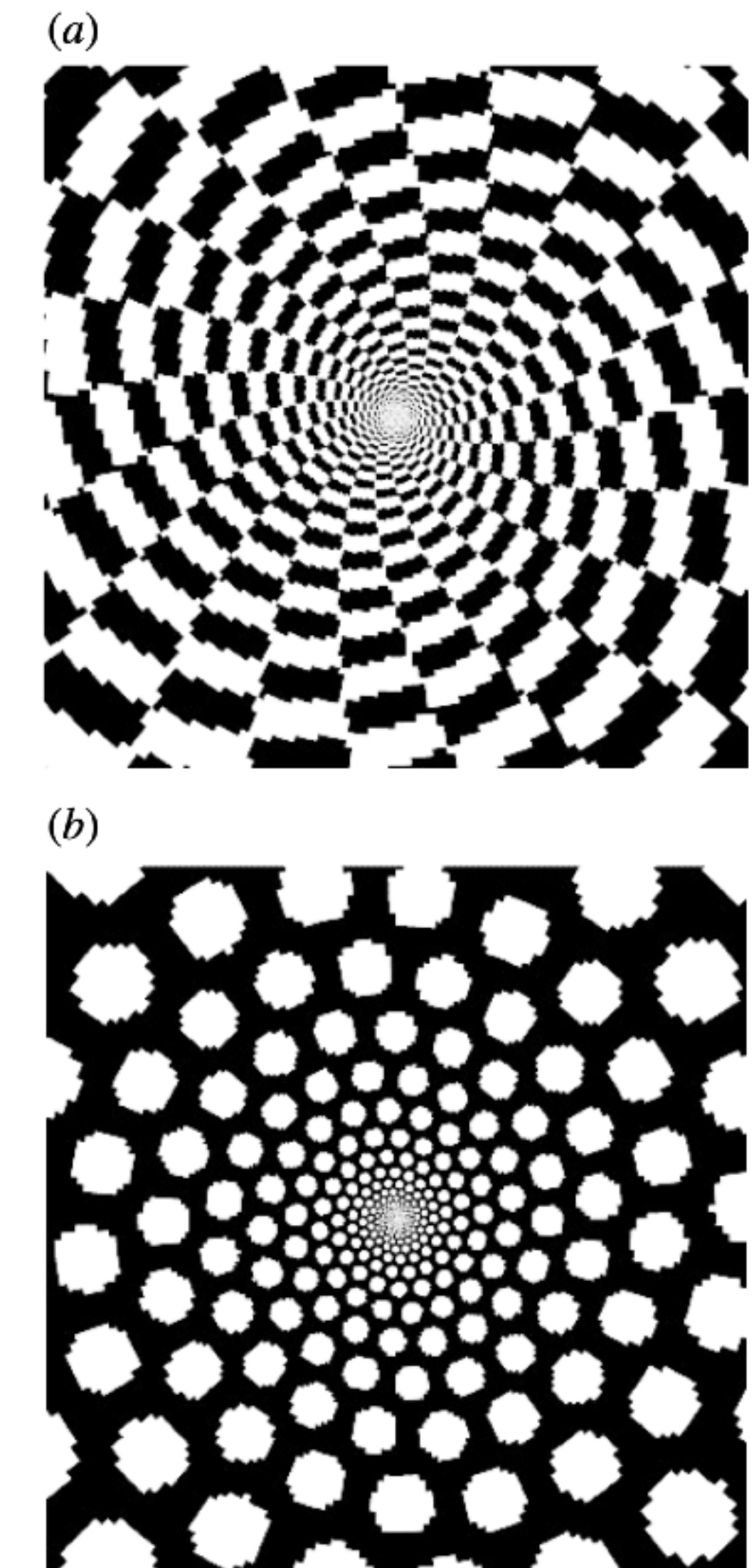


Figure 30. Action of the single inverse retinocortical map on non-contoured rhombic and hexagonal planforms:
(a) rhombic, (b) hexagonal.